3. PET in Lung Cancer

Ronald B. Workman, Jr. and R. Edward Coleman

Epidemiology

During 2005, there were approximately 172,570 new cases of lung cancer diagnosed in the United States. Although lung cancer accounts for about 13% of all new cancer cases, it is responsible for almost 28% of all cancer deaths and is the leading cause of cancer mortality for both men and women. An estimated 163,510 deaths were from lung cancer alone in 2005. Approximately 60% of those diagnosed with lung cancer die within 1 year, 75% die within 2 years, and the combined 5-year survival rate for all stages of lung cancer is only 15%. These figures have not changed substantially in almost a decade [1]. These statistics reflect the fact that the majority of cases are advanced at presentation; however, if caught early, various series have shown that surgical resection of a solitary lung cancer carries a 5-year survival rate of 40–80% [2,3].

The two main histopathologic categories for lung malignancy are small cell lung cancer (SCLC) and non-small cell lung cancer (NSCLC). In both its clinical behavior and treatment, SCLC is distinct from NSCLC. SCLC accounts for the minority (about 14%) of all lung cancer cases and is composed of poorly differentiated, rapidly growing cells with disease usually occurring centrally rather than peripherally. It metastasizes early. Management for SCLC is non-surgical, and therapy is via chemotherapy alone or in combination with radiotherapy. The majority of lung cancers are non-small cell in origin. While their classification is complex, it can be broadly broken down into the most common cell types: squamous, adenocarcinoma, and large cell. Table 3.1 provides a detailed outline of non-small cell cancer types [4].

Like most cancers, treatment for limited disease is usually surgical, with combination therapy reserved for more advanced cases depending on tumor site and patient performance status. Lung cancer is currently staged via the Tumor, Node, Metastasis (TNM) scheme devised by the American Joint Committee on Cancer. Table 3.2 provides the TNM staging classification of lung cancer. Curative surgery alone is the treatment of choice for patients with stage IA and IB disease, although inoperable early stage patients can undergo an attempt at curative radiotherapy. Surgery in combination with chemoradiation can be performed up to stage IIIA disease. For stages IIIB and IV, treatment is non-surgical and aimed more at palliation [5].

As with the other malignancies discussed in this book, there are PET reimbursement codes that have been established by the Centers for Medicare and Medicaid Services (CMS) for various covered indications [6]. In practical terms,

Table 3.1. The new World Health Organization/International Association for the Study of Lung Cancer histologic classification of non-small cell lung cancers

1. Squamous cell carcinoma
   - Papillary
   - Clear cell
   - Small cell
   - Basaloid
2. Adenocarcinoma
   - Acinar
   - Papillary
   - Bronchioloalveolar carcinoma
     - Non-mucinous
     - Mucinous
     - Mixed mucinous and non-mucinous or indeterminate cell type
   - Solid adenocarcinoma with mucin
   - Adenocarcinoma with mixed subtypes
   - Variants
     - Well-differentiated fetal adenocarcinoma
     - Mucinous ("colloid") adenocarcinoma
     - Mucinous cystadenocarcinoma
     - Signet ring adenocarcinoma
     - Clear cell adenocarcinoma
3. Large cell carcinoma
   - Variants
     - Large cell neuroendocrine carcinoma
     - Combined large cell neuroendocrine carcinoma
     - Basaloid carcinoma
     - Lymphoepithelioma-like carcinoma
     - Clear cell carcinoma
     - Large cell carcinoma with rhabdoid phenotype
4. Adenosquamous carcinoma
5. Carcinomas with pleomorphic, sarcomatoid or sarcomatous elements
   - Carcinomas with spindle and/or giant cells
   - Spindle cell carcinoma
   - Giant cell carcinoma
   - Carcinosarcoma
   - Pulmonary blastoma
6. Carcinoid tumor
   - Typical carcinoid
   - Atypical carcinoid
7. Carcinomas of salivary-gland type
   - Mucoepidermoid carcinoma
   - Adenoid cystic carcinoma
   - Others
8. Unclassified carcinoma

Source: Non-small cell lung cancer cellular classification. National Cancer Institute (www.cancer.gov); 2005 Accessed April 2005.

Table 3.2. TNM staging for lung cancer

Primary tumor (T)	
TX	Primary tumor cannot be assessed, or tumor proven by the presence of malignant cells in sputum or bronchial washings but not visualized by imaging or bronchoscopy
T0	No evidence of primary tumor
Tis	Carcinoma in situ
T1	Tumor 3 cm or less in greatest dimension, surrounded by lung or visceral pleura, without bronchoscopic evidence of invasion more proximal than the lobar bronchus* (i.e., not in the main bronchus)
T2	Tumor with any of the following features of size or extent: More than 3 cm in greatest dimension Involves main bronchus, 2 cm or more distal to the carina Invades the visceral pleura Associated with atelectasis or obstructive pneumonitis that extends to the hilar region but does not involve the entire lung
T3	Tumor of any size that directly invades any of the following: chest wall (including superior sulcus tumors), diaphragm, mediastinal pleura, parietal pericardium; or tumor in the main bronchus less than 2 cm distal to the carina, but without involvement of the carina; or associated atelectasis or obstructive pneumonitis of the entire lung
T4	Tumor of any size that invades any of the following: mediastinum, heart, great vessels, trachea, esophagus, vertebral body, carina; or separate tumor nodules in the same lobe; or tumor with a malignant pleural effusion†
Regional lymph nodes (N)	
NX	Regional lymph nodes cannot be assessed
N0	No regional lymph node metastasis
N1	Metastasis to ipsilateral peribronchial and/or ipsilateral hilar lymph nodes, and intrapulmonary nodes including involvement by direct extension of the primary tumor
N2	Metastasis to ipsilateral mediastinal and/or subcarinal lymph nodes
N3	Metastasis to contralateral mediastinal, contralateral hilar, ipsilateral or contralateral scalene, or supraclavicular lymph nodes
Distant metastasis (M)	
MX	Distant metastasis cannot be assessed
M0	No distant metastasis
M1	Distant metastasis present (includes separate tumor nodule(s) in a different lobe, ipsilateral or contralateral)

Stage grouping			
Occult carcinoma	TX	N0	M0
Stage 0	Tis	N0	M0
Stage IA	T1	N0	M0
Stage IB	T2	N0	M0
Stage IIA	T1	N1	M0

Continued.

Table 3.2. *Continued.* TNM staging for lung cancer

Stage IIB	T2	N1	M0
	T3	N0	M0
Stage IIIA	T1	N2	M0
	T2	N2	M0
	T3	N1	M0
	T3	N2	M0
Stage IIIB	Any T	N3	M0
	T4	Any N	M0
Stage IV	Any T	Any N	M1

* *Note*: the uncommon superficial tumor of any size with its invasive component limited to the bronchial wall, which may extend proximal to the main bronchus, is also classified T1.

† *Note*: Most pleural effusions associated with lung cancer are due to tumor. However, there are a few patients in whom multiple cytopathologic examinations of pleural fluid are negative for tumor. In these cases, fluid is non-bloody and is not an exudate. Such patients may be further evaluated by videothoracoscopy (VATS) and direct pleural biopsies. When these elements and clinical judgment dictate that the effusion is not related to the tumor, the effusion should be excluded as a staging element and the patient should be staged T1, T2, or T3.

Source: Used with permission of the American Joint Committee on Cancer (AJCC), Chicago, Illinois. The original source for this material is the *AJCC Cancer Staging Manual*, Sixth Edition (2002), published by Springer-Verlag, New York, www.springeronline.com.

these indications are as follows: (1) Diagnosis: Is the lesion benign or malignant? (2) Initial staging: What is the extent of disease? (3) Restaging: Is disease present after treatment? CMS was covering these indications under specific G-codes but is now using CPT codes (see Chapter 2: Reimbursement for PET and PET/CT Imaging).

Diagnosis – Fluorodeoxyglucose-Positron Emission Tomography and Evaluation of the Solitary Pulmonary Nodule

A solitary pulmonary nodule (SPN) has been defined as a single intraparenchymal opacity completely surrounded by lung without any associated atelectasis or lymph node enlargement and with a diameter less than or equal to 3 cm [7,8]. If a lesion is larger than 3 cm, it is termed a mass rather than a nodule. Such masses are almost always malignant.

The solitary pulmonary nodule is a common finding, with an estimated 130,000 nodules identified each year in the United States by plain chest radiograph. Most SPNs are benign entities such as granulomas or hamartomas. But, in patient populations at high risk for developing a primary lung cancer (e.g.

history of smoking, radon or asbestos exposure), and with nodules growing or becoming symptomatic, they are especially worrisome for malignancy. While most malignant SPNs are bronchogenic carcinomas, extrapulmonary metastatic disease accounts for 10–30% of all malignant SPNs.

Twenty to thirty percent of lung cancer patients have an SPN as their initial presentation of disease [9]. Proponents of early detection of lung cancer claim that it offers the best chance for cure [10]. Therefore, accurate and timely assessment of the SPN may be important in successful patient management.

The goal of radiologic evaluation of the SPN is to accurately differentiate benign from malignant lesions. Size, contour, margin, and calcification pattern are some of the morphologic characteristics employed in conventional radiologic analysis. Table 3.3 provides a more detailed list of the radiologic features a lesion may possess that can aid in assessing whether it is benign or malignant. Although the information gained with conventional radiography is invaluable, the vast majority of SPNs are indeterminate by plain film chest radiography and computed tomography [11–13]. In many cases, a tissue diagnosis must be obtained under imaging guidance. In cases where suspicious nodules are technically

Table 3.3. Solitary pulmonary nodule (SPN) imaging characteristics favoring benignancy or malignancy

Findings favoring a benign lesion	Findings favoring a malignant lesion
Conventional imaging with chest radiograph and/or CT	
Size less than 2 cm	Size greater than 3 cm
Stable appearance (especially for >2 years)	Interval change
Smooth margin	Spiculated, irregular, or lobulated margin
Diffuse calcification (lamellated or central calcification is typical for granulomas; “popcorn” calcification is typical for hamartomas)	Stippled or eccentric calcification
Satellite nodules (when seen at the periphery of a dominant smooth nodule this suggests an infectious granuloma)	
If cavitation is present, smooth, thin walls (i.e., 4 mm or less) favor a benign process [12]	If cavitation is present, irregular, thick walls (i.e., greater than 15 mm) favor malignancy [12]
Nodule enhancement <15 Hounsfield Units (HU) [13]	Malignant lesions are relatively hypervascular
Imaging with FDG-PET	
SUV <2.5, or visually less metabolically active than mediastinal blood pool (for nodules >1.0 cm)	SUV >2.5, or visually more metabolically active than mediastinal blood pool (for nodules >1.0 cm)

difficult to biopsy, co-morbidities make biopsy too risky, prior biopsy has been non-diagnostic or prior biopsy was negative because of sampling error and concern remains for a false-negative biopsy in a high-risk patient, FDG-PET can be used to assess the character of a pulmonary lesion without intervention. For this reason, an FDG-PET scan can be thought of as a non-invasive metabolic biopsy. For examples of FDG-PET/CT scans for evaluation of SPN, see Figures 3.1 and 3.2.

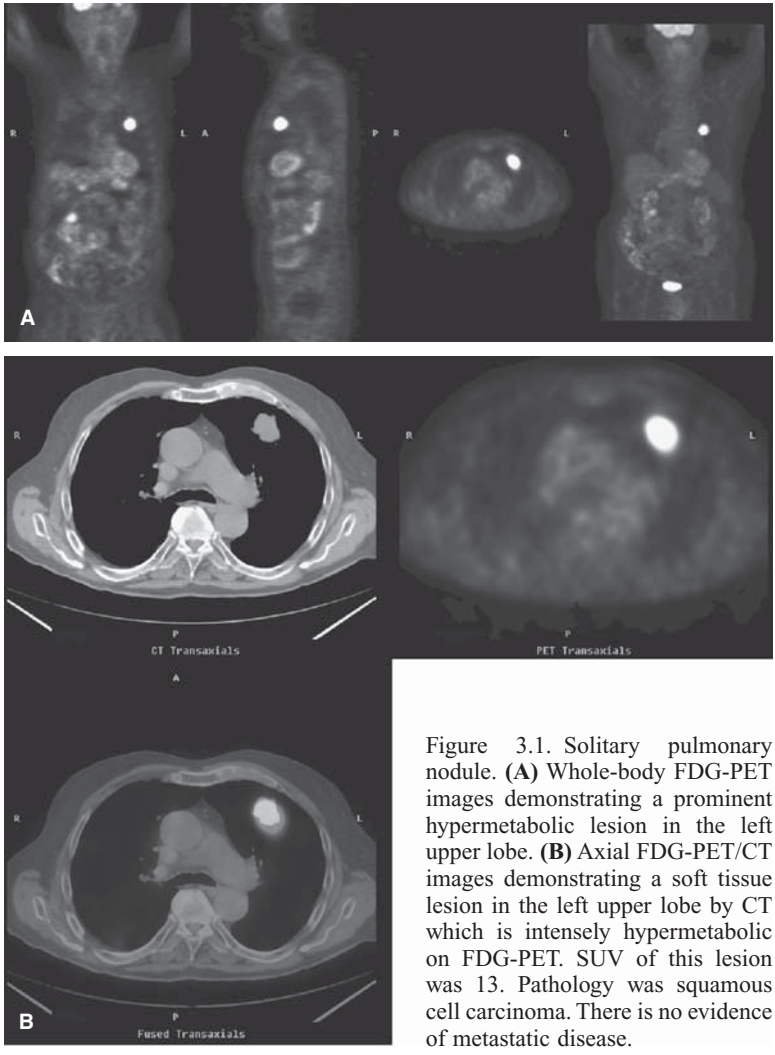

Figure 3.1. Solitary pulmonary nodule. **(A)** Whole-body FDG-PET images demonstrating a prominent hypermetabolic lesion in the left upper lobe. **(B)** Axial FDG-PET/CT images demonstrating a soft tissue lesion in the left upper lobe by CT which is intensely hypermetabolic on FDG-PET. SUV of this lesion was 13. Pathology was squamous cell carcinoma. There is no evidence of metastatic disease.

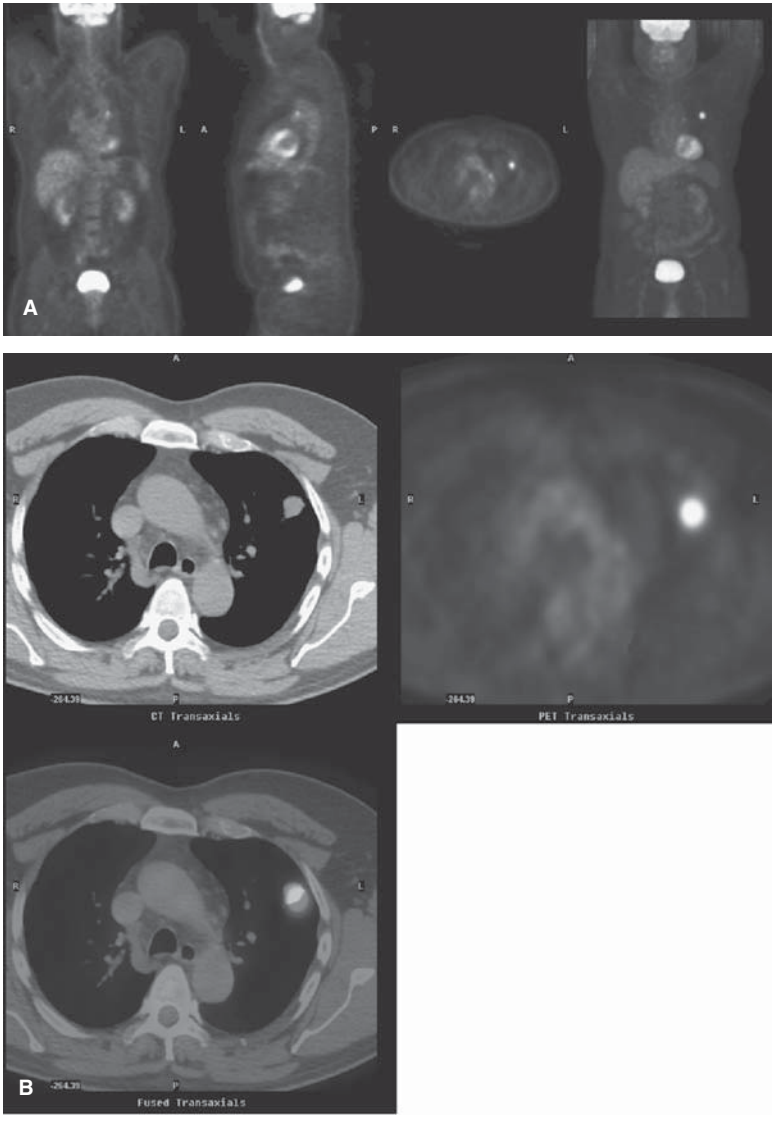

Figure 3.2. Solitary pulmonary nodule with ipsilateral hilar metastasis. **(A)** FDG-PET whole-body scan of another patient with a suspicious left upper lobe nodule which is hypermetabolic (SUV = 6) and highly suspicious for malignancy. A faint focus of increased activity is seen in the left hilar region. **(B)** Axial FDG-PET/CT images through the left upper lobe lesion demonstrate hypermetabolism consistent with malignancy.

Continued.

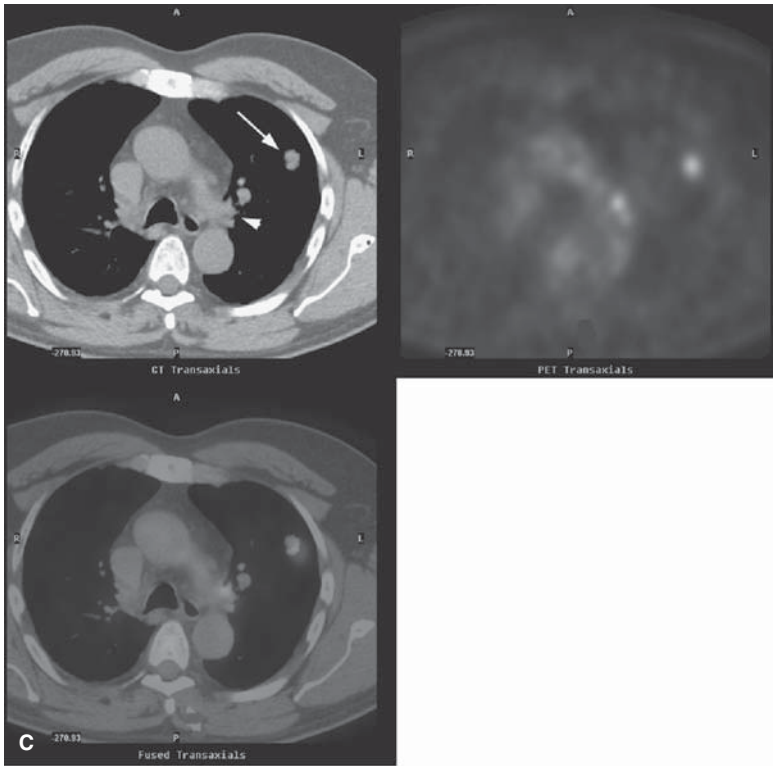

Figure 3.2. *Continued.* **(C)** Additional axial images slightly more inferiorly again demonstrate the hypermetabolic left upper lobe lesion (white arrow). There is increased focal uptake in the left hilar region consistent with metastatic adenopathy (white arrowhead).

Standardized Uptake Value and the Solitary Pulmonary Nodule

Since the 1920s, biochemists have demonstrated that cancers are more metabolically active than normal tissue. To support this hypermetabolism, cancer cells have increased uptake and utilization of glucose. As discussed in Chapter 1, the standardized uptake value (SUV) is a semi-quantitative measure of the relative degree of FDG metabolism within a lesion of interest. While there are certain important limitations that will be addressed later in this chapter, in general, an SUV greater than 2.5 is an indicator of malignancy [14–16]. Visually, when the metabolic activity of the lesion is greater than that seen within

the mediastinum (often called mediastinal blood pool activity) it is also considered malignant.

The degree of FDG accumulation within a primary lesion has been shown to have prognostic value. The SUV within an SPN inversely correlates with the lesion's doubling time (i.e., the time required for a tumor to double in volume). The higher the SUV, the shorter the doubling time. For lesions that have an SUV less than 10, median patient survival is approximately 24 months. In lesions with an SUV greater than 10, median survival is only about 11 months. If a nodule is greater than 3 cm in diameter and the SUV is greater than 10, median survival is 6 months. Several studies have reported similar results [17].

Accuracy of Fluorodeoxyglucose-Positron Emission Tomography in Lung Cancer Diagnosis

In 2001, the *Journal of the American Medical Association* published a comprehensive meta-analysis of the accuracy of FDG-PET in diagnosing pulmonary nodules and mass lesions. The authors compiled data from the previous 4 years of work, and selected 40 studies for inclusion. Based on their analysis of almost 1500 total focal pulmonary lesions, FDG-PET scanning had a sensitivity of 96.8% and a specificity of 77.8% [18].

Fluorodeoxyglucose-Positron Emission Tomography in Lung Cancer Staging

FDG-PET and FDG-PET/CT are whole-body scans. In patients with biopsy-proven, non-small cell lung cancer, FDG-PET is the most accurate, non-invasive method for staging the entire body with the exception of the brain. (For an in-depth discussion of FDG-PET in evaluating intracranial metastatic disease, see Chapter 13, PET in Neurology.) In one study, investigators took 100 patients with newly diagnosed bronchogenic carcinoma and compared FDG-PET staging with that of chest CT, bone scan, and contrast-enhanced CT or magnetic resonance imaging (MRI) of the brain [19]. Radiologic staging with FDG-PET and conventional imaging using chest CT, bone scintigraphy with ^{99m}Tc methylene diphosphonate (MDP), and brain CT or MRI were compared with pathologic stage. In overall staging, FDG-PET was accurate in 83%, compared to 65% for conventional imaging ($P < 0.005$). Staging of mediastinal lymph nodes was accurate in 85%, compared to 58% with conventional imaging ($P < 0.001$). Nine percent of patients had metastases detected with FDG-PET that were not identified by conventional imaging, and conversely 10% of patients suspected of having metastatic disease by conventional imaging were correctly shown by FDG-PET to be free of metastatic disease. In unresectable (N3) disease the sensitivity and specificity of FDG-PET were 92% and 93%, respectively, compared to sensitivity and specificity of 25% and 98% for CT. FDG-PET was also

superior in correctly identifying those patients with metastatic (i.e., M1) disease in 91% versus 80% for conventional imaging.

FDG-PET is superior to bone scintigraphy for detecting osseous metastatic disease from bronchogenic carcinoma, with a sensitivity and specificity of 92% and 99%, respectively, compared to a sensitivity and specificity of 50% and 92%, respectively, with bone scan [19]. More recent research comparing bone scintigraphy using ^{99m}Tc MDP and FDG-PET in retrospective staging of newly diagnosed lung cancer patients has echoed these earlier results and further suggests that bone scintigraphy can be eliminated from the initial work-up since it provides redundant and less accurate information compared to FDG-PET [20]. In practice, bone scintigraphy is likely to remain commonplace in oncologic imaging for the foreseeable future because of its long record of high accuracy as well as its ready availability, and familiarity compared to FDG-PET, especially in communities that may not be able to support PET equipment and personnel.

Once whole-body scanning with FDG-PET has excluded distant metastatic disease, staging of the mediastinum is critical to determine lesion resectability thereby maximizing the chance for cure. Although the gold standard for staging the mediastinum remains mediastinoscopy, FDG-PET offers vital information. In a report published in 2003, researchers retrospectively studied 400 patients with NSCLC. Each patient underwent a CT scan of the chest and upper abdomen as well as an FDG-PET scan 1 month before planned surgery. All suspicious N2 lymph nodes by either chest CT or FDG-PET scan were biopsied. Patients without malignant involvement of mediastinal or distant nodes and without metastasis underwent pulmonary resection and complete thoracic lymphadenectomy. Results demonstrated that FDG-PET had a higher sensitivity (71% vs. 43%, $P < 0.001$), positive predictive value (44% vs. 31%, $P < 0.001$), negative predictive value (91% vs. 84%, $P = 0.006$), and accuracy (76% vs. 68%, $P = 0.037$) than CT scan for N2 lymph nodes. Similarly, FDG-PET had a higher sensitivity (67% vs. 41%, $P < 0.001$), but lower specificity (78% vs. 88%, $P = 0.009$) than CT scan for N1 lymph nodes. FDG-PET led to unnecessary mediastinoscopy in 38 patients (10%). FDG-PET was most commonly falsely negative for nodes located in the subcarinal region and the aortopulmonary window. It accurately upstaged 28 patients (7%) with unsuspected metastasis and accurately downstaged 23 patients (6%) [21]. A meta-analysis conducted in 1999 of 14 FDG-PET studies and 29 CT studies demonstrated an overall diagnostic accuracy of 92% for FDG-PET and 75% for CT in staging the mediastinum [22].

FDG-PET is more accurate than CT alone in staging the mediastinum. A positive finding in the mediastinum on FDG-PET warrants mediastinoscopy with tissue biopsy at that location. Also, the use of FDG-PET in initial staging improves patient selection by eliminating those with unsuspected metastatic or unresectable disease from undergoing futile therapy. A recent meta-analysis concluded that unexpected extrathoracic metastatic disease is seen in as many as 12% of patients undergoing FDG-PET [23]. However, an FDG-PET scan that is positive for distant metastatic disease should be confirmed by undergoing directed biopsy of the probable metastasis in order to avoid excluding a patient from potentially curative therapy. See Figures 3.3, 3.4 and 3.5 for examples of staging FDG-PET/CT scans.

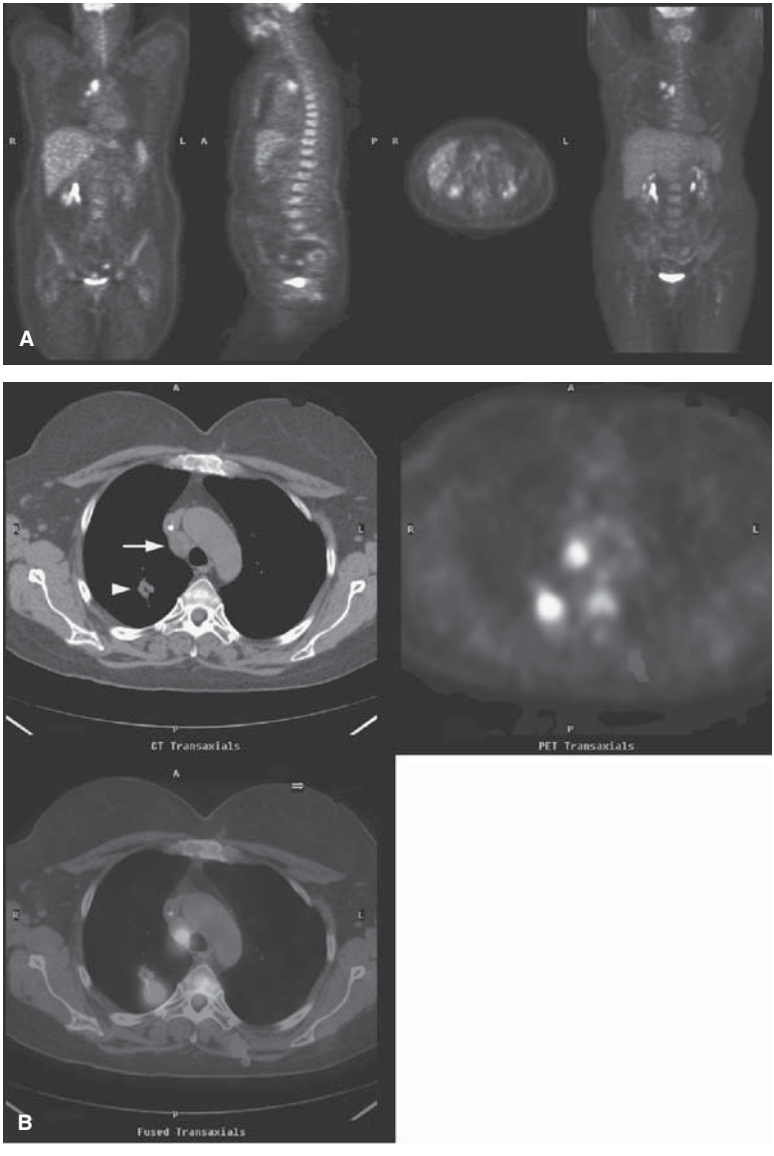

Figure 3.3. Right upper lobe NSCLC with ipsilateral metastatic adenopathy and a benign left adrenal adenoma. **(A)** FDG-PET whole-body scan demonstrating a right hilar malignancy with ipsilateral metastatic adenopathy. No evidence of distant disease is seen. **(B)** Axial FDG-PET/CT image through the right upper lobe lesion (white arrowhead) and the right paratracheal nodal metastasis (white arrow). Also notice the slight image misregistration.

Continued.

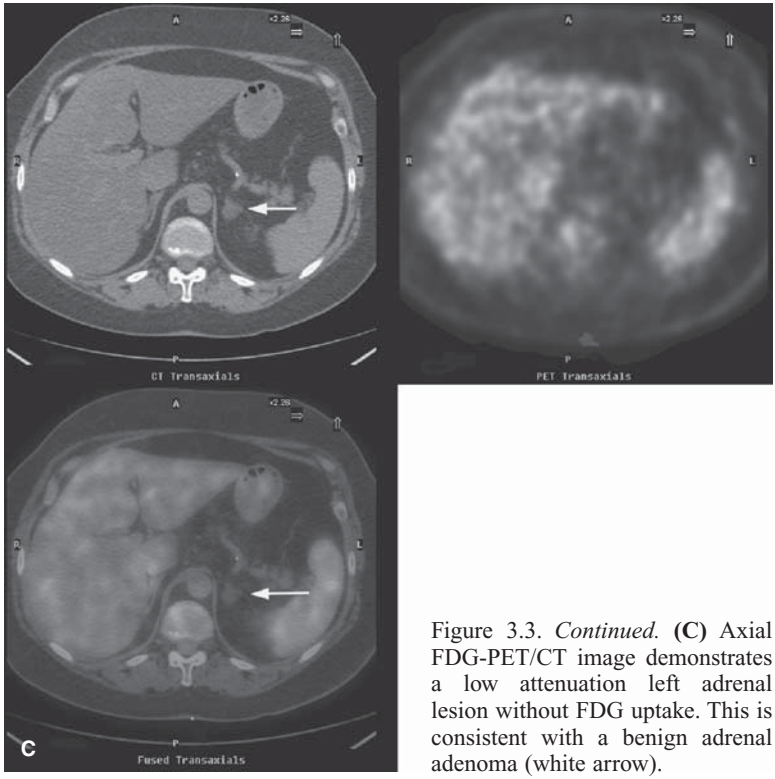

Figure 3.3. *Continued.* **(C)** Axial FDG-PET/CT image demonstrates a low attenuation left adrenal lesion without FDG uptake. This is consistent with a benign adrenal adenoma (white arrow).

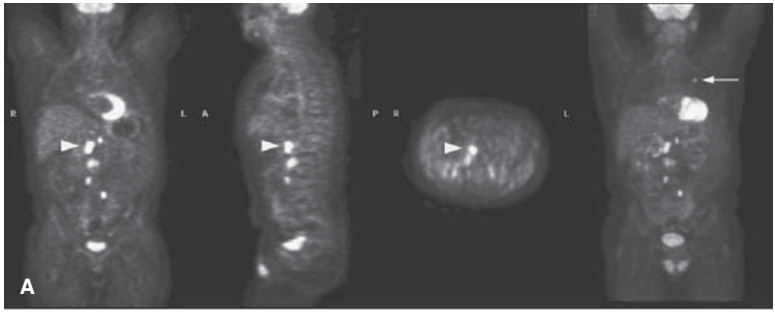

Figure 3.4. Left upper lobe NSCLC with distant metastases. **(A)** FDG-PET whole-body image demonstrating a left upper lobe malignancy (white arrow) with right adrenal metastasis (white arrowhead). Additional metastases are seen in the retroperitoneum.

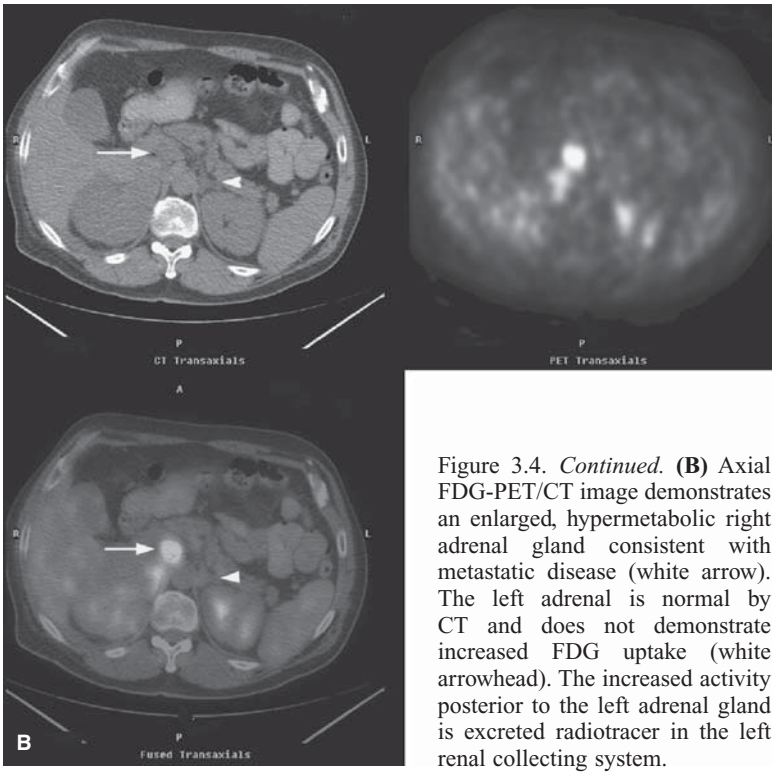

Figure 3.4. *Continued.* **(B)** Axial FDG-PET/CT image demonstrates an enlarged, hypermetabolic right adrenal gland consistent with metastatic disease (white arrow). The left adrenal is normal by CT and does not demonstrate increased FDG uptake (white arrowhead). The increased activity posterior to the left adrenal gland is excreted radiotracer in the left renal collecting system.

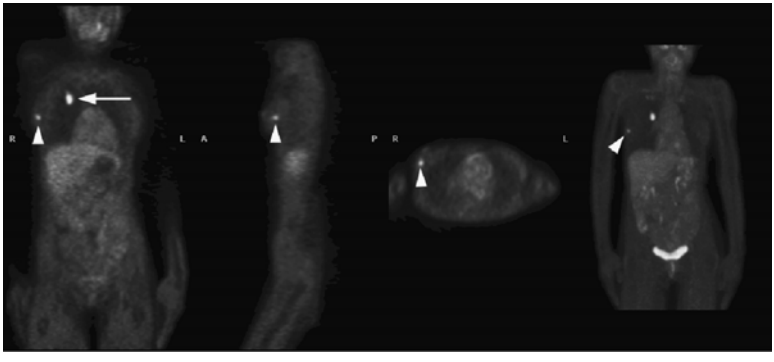

Figure 3.5. Lung cancer staging scan with incidental second primary. FDG-PET whole-body scan of a patient with NSCLC of the right mid lung (white arrow). In this case, an additional hypermetabolic lesion was detected in the lower outer quadrant of the right breast (white arrowhead). Subsequent biopsy confirmed the lesion to be a breast primary.

Fluorodeoxyglucose-Positron Emission Tomography in Lung Cancer Restaging

FDG-PET has an important role in monitoring for recurrence and in evaluating the effects of treatment. Because FDG-PET gauges metabolic activity, treated disease can be evaluated on the basis of its physiology in addition to the morphologic assessment provided by CT. FDG-PET is more accurate than CT in differentiating between post-therapy change and residual or recurrent disease. In one study of 126 patients with stage I–IIIB disease treated with radiation therapy, FDG-PET had a sensitivity and specificity of 100% and 92%, respectively, in detecting active disease. Positive and negative predictive values were 92% and 100%, respectively. By comparison, CT had a sensitivity and specificity of 72% and 95%, respectively, and positive and negative predictive values of 93% and 79%, respectively [24].

FDG-PET scanning following therapy also has prognostic value. The response to therapy can be classified as complete remission, partial remission, no response, or progression of disease. In 2003, MacManus et al. examined 73 patients who underwent radical radiotherapy or chemoradiotherapy followed by FDG-PET at 10 weeks. Each patient had a determination made as to response to therapy based on both CT and FDG-PET, and these responses were then correlated with survival. The response to therapy determined by FDG-PET was found to be superior to CT in predicting survival duration [25]. In another recent study of 56 patients, the change in the maximum SUV (SUV_{max}) within a lesion on FDG-PET scan after neoadjuvant therapy was found to hold a near linear relationship with pathologic response and was a more accurate predictor than was the change in lesion size on CT scan. This study found that when the SUV_{max} decreases by 80% or more there is a high likelihood (with 96% accuracy), that the patient is a complete responder irrespective of cell type, neoadjuvant treatment, or the final absolute SUV_{max} [26]. See Figures 3.6 and 3.7 for examples of restaging studies (see also Plate 3.6B, in the color insert).

Figure 3.6. Recurrence adjacent to radiation therapy field. **(A)** FDG-PET whole-body images from a patient with a history of metastatic lung cancer. The patient is status post radiation therapy to the left upper lobe. Multiple metastatic foci are seen in distant sites including the axial and proximal appendicular skeleton. **(B)** Axial images demonstrate intense FDG uptake at the anterior margin of the radiation therapy field consistent with tumor recurrence (white arrow). Notice the less intense diffuse uptake in the remainder of the treated lung consistent with inflammatory post-therapy changes (white arrowhead). (See part B only in the color insert.)

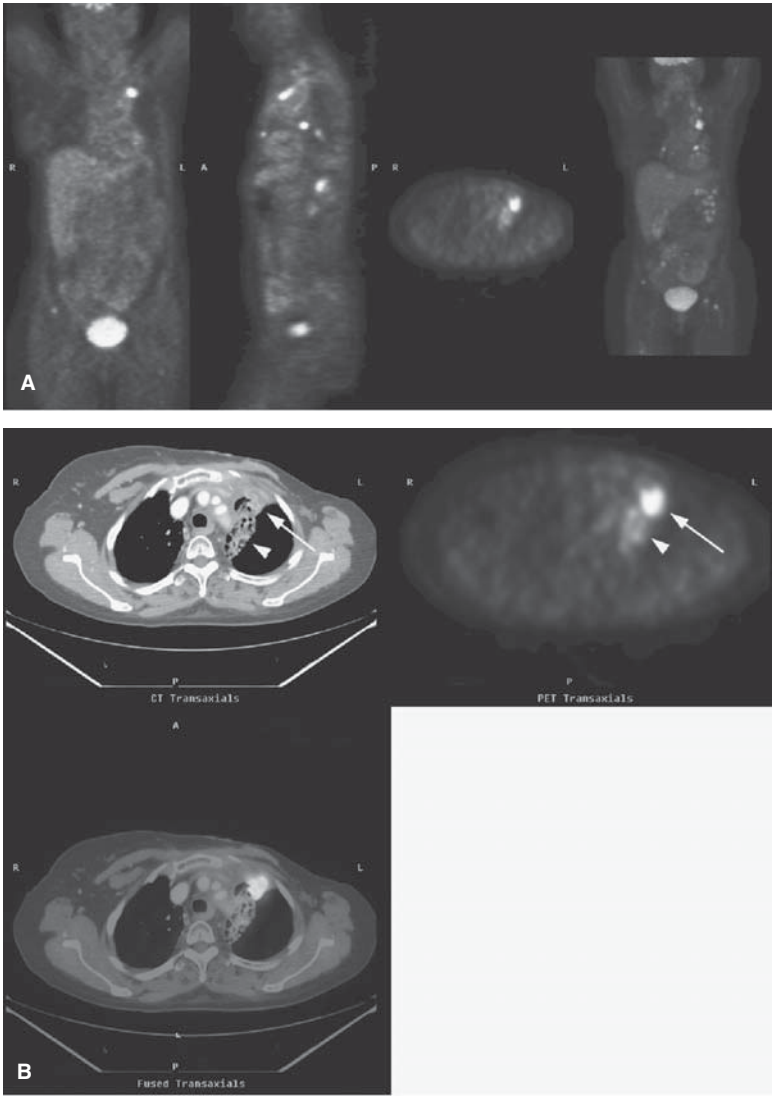
A
B
CT Transaxials
PET Transaxials
Fused Transaxials

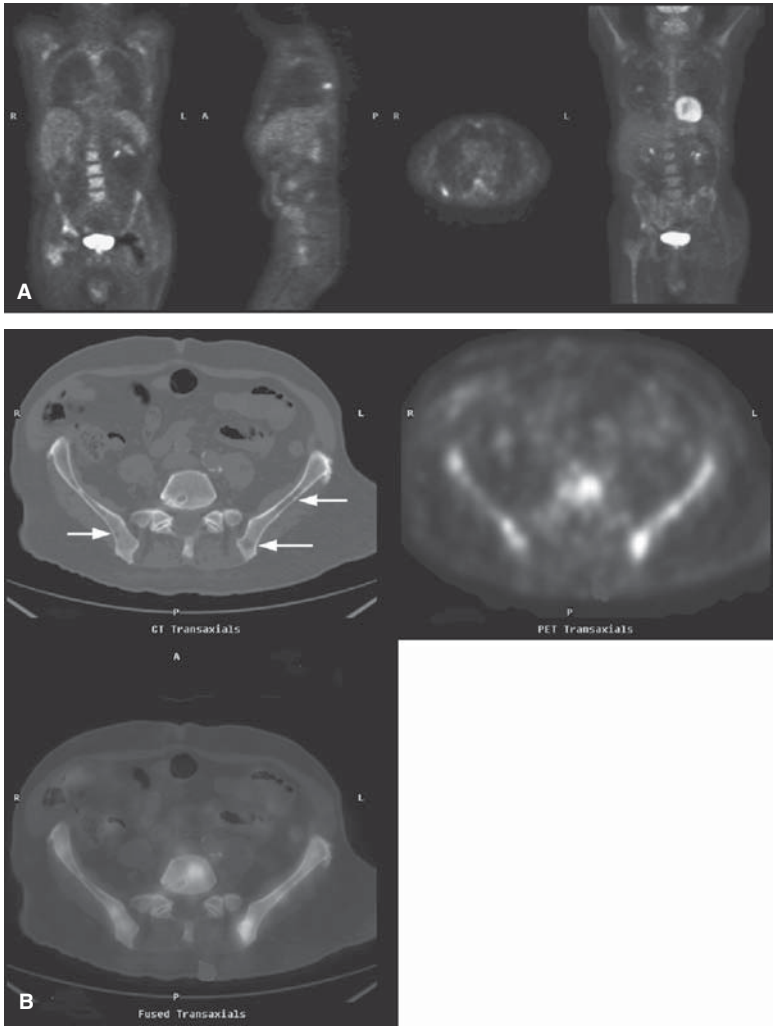

Figure 3.7. Skeletal metastatic disease in the setting of reactive marrow. **(A)** FDG-PET whole-body images demonstrate moderate diffuse FDG uptake in the bone marrow. This can be seen in patients undergoing chemotherapy, as a response to anemia, or following colony-stimulating factors. In this patient, however, there are foci of increased activity best seen in a right rib and within the pelvis consistent with skeletal metastatic disease. Also notice the photopenic left hip prosthesis on the coronal image. **(B)** Axial images demonstrate several lytic lesions in the bony pelvis (white arrows) with corresponding hypermetabolism. Notice the diffuse, less intense FDG uptake elsewhere in bones likely represents physiologic marrow recruitment changes.

Fluorodeoxyglucose-Positron Emission Tomography/Computed Tomography in Lung Cancer

With the increasing prevalence of hybrid FDG-PET/CT systems, imaging specialists can offer clinicians more accurate information than can be obtained by either PET or CT alone. In 2003, Lardinois et al. prospectively looked at 50 patients with proven or suspected NSCLC and compared the accuracy of PET/CT with that of PET alone, CT alone, and with visually correlated PET and CT scans obtained separately (i.e., not obtained simultaneously with an integrated PET/CT system). Imaging stage was then compared with pathologic stage. Their results, published in the *New England Journal of Medicine*, demonstrated that integrated PET/CT provided additional information in 20 of 49 patients (41%), beyond that provided by conventional visual correlation of PET and CT. Furthermore, integrated PET/CT had better diagnostic accuracy than the other imaging methods. Tumor staging was significantly more accurate with integrated PET/CT than with CT alone ($P = 0.001$), PET alone ($P < 0.001$), or visual correlation of PET and CT ($P = 0.013$); node staging was also significantly more accurate with integrated PET/CT than with PET alone ($P = 0.013$). In evaluating for metastasis, integrated PET/CT increased the diagnostic certainty in two of eight patients [27].

Specifically, integrated PET/CT was helpful in clarifying the extent of the primary tumor (i.e., T stage), particularly in determining whether there was chest wall invasion. PET/CT was also helpful in clarifying mediastinal invasion and pinpointing nodal involvement within the mediastinum, hila, and supraclavicular regions because precise node localization is not possible with PET alone. In this study, software fusion of PET with CT (as opposed to integrated PET/CT) was no better than PET alone. FDG-PET/CT is poised to be the single most powerful radiologic examination in evaluating the lung cancer patient. New advances in hybrid scanner technology, PET scanner resolution, and intravenous contrast protocols for the CT portion of the study should further improve diagnostic accuracy and patient care.

Not only does FDG-PET/CT improve diagnostic accuracy, it also improves the ability of radiation oncologists to more accurately target diseased tissue in their planning. In those patients who are to undergo preoperative radiation therapy or palliation radiotherapy, FDG-PET/CT allows for much more precise delineation of tumor target volumes with the use of the fused (i.e., registered) PET and CT images. Use of PET/CT fusion images has the potential to reduce irradiation of non-diseased, non-target organs, to reduce the incidence of geographic misses, and to improve the radiation oncologist's understanding of tumor metabolism and biology [28].

Some institutions do not use intravenous or oral contrast for the CT scans performed in the evaluation of suspected or documented lung cancer. For these patients, the CT scan performed with the PET/CT can be obtained as a diagnostic CT scan if ordered by the referring clinician. Furthermore, several centers are now performing contrast-enhanced CT scans when ordered with the PET/CT scan, and these can be obtained sequentially on the PET/CT scanner.

Limitations

Lesion size is an important factor when a patient is undergoing FDG-PET evaluation for lung cancer. The threshold for lesion detection for most FDG-PET scanners currently in use is between 6 and 8 mm. As a rule, for lesions that are greater than 1 cm, an SUV greater than or equal to 2.5 or a visual intensity greater than that within the mediastinal blood pool are accepted criteria for malignancy. Any activity seen within a nodule less than 1 cm is suspicious. The smaller the lesion, the greater is the likelihood of a false-negative scan because of volume averaging with surrounding normal tissue. Other important causes of a false-negative FDG-PET scan are well-differentiated cancers such as bronchioloalveolar carcinoma (BAC), slow growing neuroendocrine tumors such as bronchial carcinoid (Figure 3.8), and mucinous neoplasms.

As discussed throughout this book and throughout the FDG-PET literature, not all that is hypermetabolic is cancer. Infectious and inflammatory processes aggregate metabolically active macrophages which also have increased glucose demand and can cause false-positive results on an FDG-PET scan. Some examples of false positives include cases of granulomatous infection, fungal infection, sarcoidosis, radiation-induced lung injury, pneumonitis/pneumonia, talc pleurodesis, and recent surgery/trauma. For an example of a patient who has had talc pleurodesis, see Figure 3.9. To offset some of these limitations, several

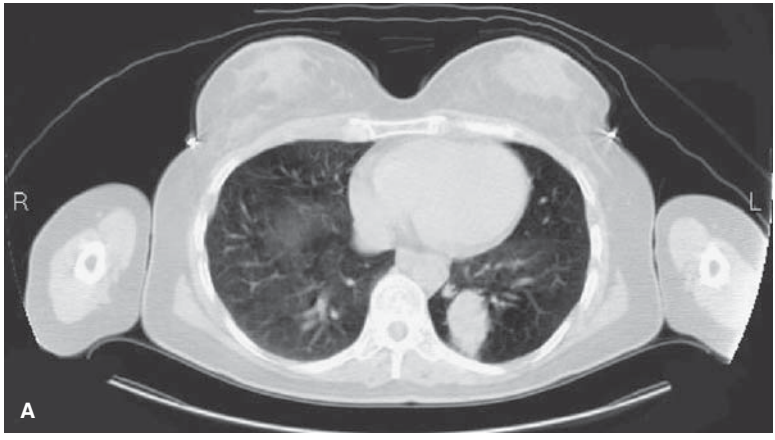

Figure 3.8. Bronchial carcinoid **(A** and **B)**. FDG-PET/CT images demonstrate a mass measuring 3.5 × 2.7 cm in the left lower lobe. The mass has an SUV of 2.1 and is similar in intensity to the activity of the mediastinal blood pool. This degree of activity, although non-specific, suggests a benign inflammatory etiology. The patient subsequently underwent resection and surgical pathology revealed well-differentiated neuroendocrine carcinoma with endobronchial extension. (Case courtesy of Ronald B. Workman, Sr., MD.)

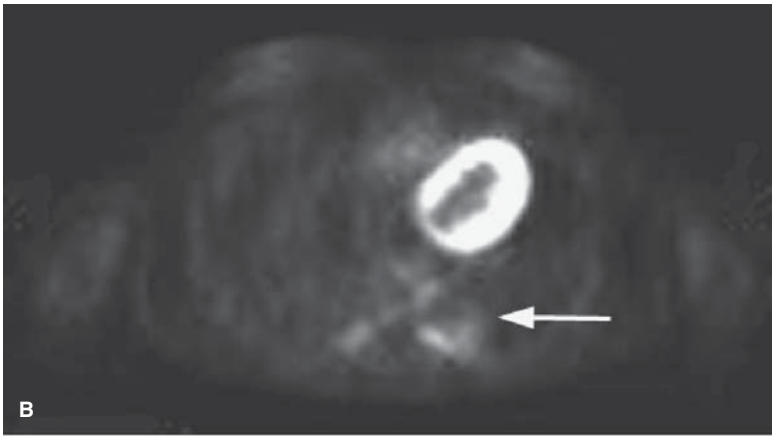

Figure 3.8. *Continued.*

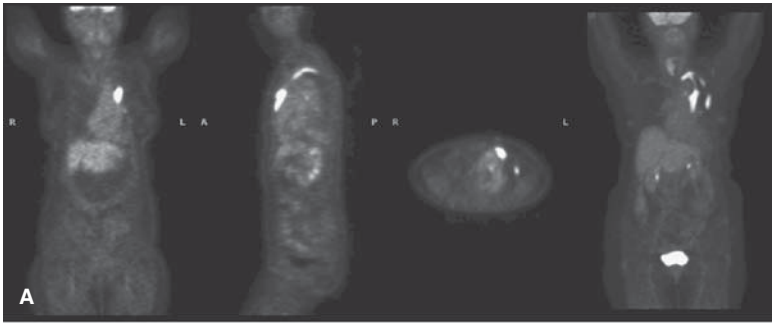

Figure 3.9. Intense FDG uptake associated with talc pleurodesis. **(A)** Whole-body FDG-PET images demonstrate intense focal uptake along the margin of the left upper lung. By PET alone, and without important history, this would be consistent with malignancy. Incidentally noted is diffuse activity in the right lobe of the thyroid (in the maximum intensity projection image on the right). This was stable compared to the patient's prior scans and was felt to represent chronic thyroiditis. **(B)** Axial FDG-PET/CT images reveal high attenuation pleural thickening with corresponding intense hypermetabolism along the anterior and anterolateral surface of the left lung (white arrows). This is consistent with chronic pleural inflammation following talc pleurodesis. Surgical clips from left upper lobectomy are also seen in the left hilum. The low level uptake in the left hilum likely represents reaction to chronic pleural inflammation.

Continued.

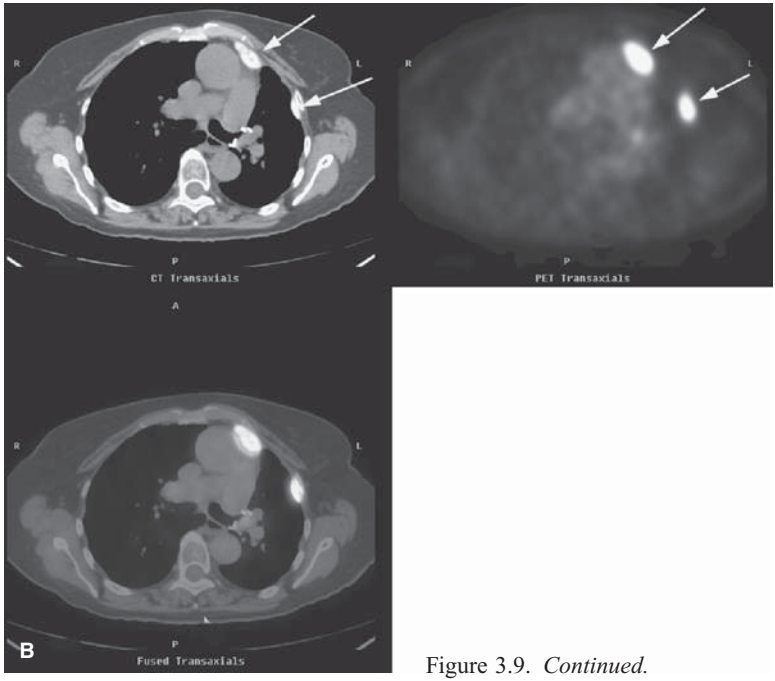

Figure 3.9. *Continued.*

researchers have conducted studies based on the observation that as a rule, malignancies demonstrate a continually increasing uptake of FDG whereas inflammatory lesions do not [29,30]. So-called dual-time point FDG-PET scanning at 1 and 2 hours after FDG administration can be performed with excellent sensitivity and specificity in the detection of malignant pulmonary nodules [31]. The advantage of dual-time point imaging over that of first imaging at 2 hours after FDG administration has not been demonstrated.

References

1. What are the key statistics for lung cancer? American Cancer Society (www.cancer.org); 2005 Accessed March 2005.
2. Mountain CF. Revisions in the International System for Staging Lung Cancer. Chest 1997;111(6):1710–1717.
3. Suzuki K, Nagai K, Yoshida J, et al. Prognostic factors in clinical stage I non-small cell lung cancer. Ann Thorac Surg 1999;67(4):927–932.
4. Non-small cell lung cancer cellular classification. National Cancer Institute (www.cancer.gov); 2005 Accessed April 2005.

5. Greene FL, Page DL, Fleming ID, et al. AJCC Cancer Staging Manual, sixth edition. New York: Springer-Verlag; 2002.
6. Medicare Coverage Homepage. Centers for Medicare and Medicaid Services (www.cms.hhs.gov/coverage/); 2005 Accessed April 2005.
7. Leef JL, 3rd, Klein JS. The solitary pulmonary nodule. Radiol Clin North Am 2002; 40(1):123–143, ix.
8. Midthun DE, Swensen SJ, Jett JR. Approach to the solitary pulmonary nodule. Mayo Clin Proc 1993;68(4):378–385.
9. Viggiano RW, Swensen SJ, Rosenow EC, 3rd. Evaluation and management of solitary and multiple pulmonary nodules. Clin Chest Med 1992;13(1):83–95.
10. Henschke CI, Yankelevitz DF, Kostis WJ. CT screening for lung cancer. Semin Ultrasound CT MR 2003;24(1):23–32.
11. Gurney JW, Lyddon DM, McKay JA. Determining the likelihood of malignancy in solitary pulmonary nodules with Bayesian analysis. Part II. Application. Radiology 1993;186(2):415–422.
12. Woodring JH, Fried AM, Chuang VP. Solitary cavities of the lung: diagnostic implications of cavity wall thickness. AJR Am J Roentgenol 1980;135(6):1269–1271.
13. Swensen SJ, Viggiano RW, Midthun DE, et al. Lung nodule enhancement at CT: multicenter study. Radiology 2000;214(1):73–80.
14. Lowe VJ, Hoffman JM, DeLong DM, Patz EF, Coleman RE. Semiquantitative and visual analysis of FDG-PET images in pulmonary abnormalities. J Nucl Med 1994; 35(11):1771–1776.
15. Lowe VJ, Fletcher JW, Gobar L, et al. Prospective investigation of positron emission tomography in lung nodules. J Clin Oncol 1998;16(3):1075–1084.
16. Goldsmith SJ, Kostakoglu L. Role of nuclear medicine in the evaluation of the solitary pulmonary nodule. Semin Ultrasound CT MR 2000;21(2):129–138.
17. Ahuja V, Coleman RE, Herndon J, Patz EF, Jr. The prognostic significance of fluorodeoxyglucose positron emission tomography imaging for patients with nonsmall cell lung carcinoma. Cancer 1998;83(5):918–924.
18. Gould MK, Maclean CC, Kuschner WG, Rydzak CE, Owens DK. Accuracy of positron emission tomography for diagnosis of pulmonary nodules and mass lesions: a meta-analysis. JAMA 2001;285(7):914–924.
19. Marom EM, McAdams HP, Erasmus JJ, et al. Staging non-small cell lung cancer with whole-body PET. Radiology 1999;212(3):803–809.
20. Cheran SK, Herndon JE, 2nd, Patz EF, Jr. Comparison of whole-body FDG-PET to bone scan for detection of bone metastases in patients with a new diagnosis of lung cancer. Lung Cancer 2004;44(3):317–325.
21. Cerfolio RJ, Ojha B, Bryant AS, Bass CS, Bartalucci AA, Mountz JM. The role of FDG-PET scan in staging patients with nonsmall cell carcinoma. Ann Thorac Surg 2003;76(3):861–866.
22. Dwamena BA, Sonnad SS, Angobaldo JO, Wahl RL. Metastases from non-small cell lung cancer: mediastinal staging in the 1990s – meta-analytic comparison of PET and CT. Radiology 1999;213(2):530–536.
23. Hellwig D, Ukena D, Paulsen F, Bamberg M, Kirsch CM. [Meta-analysis of the efficacy of positron emission tomography with F-18-fluorodeoxyglucose in lung tumors.

Basis for discussion of the German Consensus Conference on PET in Oncology 2000]. Pneumologie 2001;55(8):367–377.
24. Bury T, Corhay JL, Duysinx B, et al. Value of FDG-PET in detecting residual or recurrent nonsmall cell lung cancer. Eur Respir J 1999;14(6):1376–1380.
25. MacManus MP, Hicks RJ, Matthews JP, et al. Positron emission tomography is superior to computed tomography scanning for response-assessment after radical radiotherapy or chemoradiotherapy in patients with non-small-cell lung cancer. J Clin Oncol 2003;21(7):1285–1292.
26. Cerfolio RJ, Bryant AS, Winokur TS, Ohja B, Bartolucci AA. Repeat FDG-PET after neoadjuvant therapy is a predictor of pathologic response in patients with non-small cell lung cancer. Ann Thorac Surg 2004;78(6):1903–1909; discussion 1909.
27. Lardinois D, Weder W, Hany TF, et al. Staging of non-small-cell lung cancer with integrated positron-emission tomography and computed tomography. N Engl J Med 2003;348(25):2500–2507.
28. Ciernik IF, Dizendorf E, Baumert BG, et al. Radiation treatment planning with an integrated positron emission and computer tomography (PET/CT): a feasibility study. Int J Radiat Oncol Biol Phys 2003;57(3):853–863.
29. Gupta N, Gill H, Graeber G, Bishop H, Hurst J, Stephens T. Dynamic positron emission tomography with F-18 fluorodeoxyglucose imaging in differentiation of benign from malignant lung/mediastinal lesions. Chest 1998;114(4):1105–1111.
30. Zhuang H, Pourdehnad M, Lambright ES, et al. Dual time point 18F-FDG PET imaging for differentiating malignant from inflammatory processes. J Nucl Med 2001; 42(9):1412–1417.
31. Matthies A, Hickeson M, Cuchiara A, Alavi A. Dual time point 18F-FDG PET for the evaluation of pulmonary nodules. J Nucl Med 2002;43(7):871–875.